EPJ Web of Conferences **386**, 01002 (2026) https://doi.org/10.1051/epjconf/202638601002
XLVII Symposium on Nuclear Physics 2026

Probing Cluster Structures and Isospin Symmetry in Light Nuclei via Symmetric ^{10}B + ^{10}B Reactions

Deša Jelavić Malenica[1,*], *Matko* Milin[2], *A.* Di Pietro[3], *P.* Figuera[3], *A.* Musumarra[3], *M.G.* Pellegriti[3], *V.* Scuderi[3], *N.* Soić[1], *S.* Szilner[1], *D.* Torresi[3], and *M.* Uroić[1]

[1]Division of Experimental Physics, Ruđer Bošković Institute, Zagreb, Croatia
[2]Physics Department, Faculty of Science, University of Zagreb, Zagreb, Croatia
[3]INFN – Laboratori Nazionali del Sud and Sezione di Catania, Catania, Italy

Abstract. Measurements of the symmetric ^{10}B + ^{10}B reaction at beam energies of 50 and 72 MeV were performed at INFN - LNS. Owing to the large intrinsic spin of both projectile and target ($J^\pi = 3^+$), this reaction favors the population of high-spin states and provides efficient access to mirror nuclear systems such as ^{10}Be - ^{10}C, ^{11}B - ^{11}C, and ^{9}Be - ^{9}B. High-resolution charged-particle coincidence data allowed the reconstruction of weakly populated and previously unobserved states, offering new insight into clustering phenomena and mirror symmetry in light nuclei. Mirror spectra exhibit systematic Coulomb-shift behavior, distinguishing compact shell-model states from near-threshold cluster configurations.
Apart from mirror nuclei, in ^{12}C, a level at E_x = 24.4 MeV is strongly populated in triple-α coincidences, while in ^{13}C there is a pronounced structure at E_x = 19.0 MeV, observed in α+^{9}Be coincidences. These measurements form part of a broader program of symmetric light-ion reactions aimed at exploring clustering and shell mixing in light nuclei.

1 Introduction

Light nuclei in the $A \approx 10$ mass region exhibit a remarkable diversity of structural phenomena, ranging from conventional shell-model configurations to strongly deformed molecular and cluster states [1–4]. Rotational bands built on cluster configurations are a prominent feature of several nuclei in this mass range and often display properties that cannot be captured within a simple structural picture appropriate for light systems with a relatively small number of nucleons [5–7]. The identification of high-spin states is, of course, experimentally challenging due to the high level density at elevated excitation energies, yet it remains essential for extracting moments of inertia and constraining the structure and spatial extension of the states involved [8, 9]. Furthermore, this region is accessible not only to cluster and molecular models [10, 11] but also to modern *ab initio* approaches, providing an important bridge between detailed experimental data and first-principles nuclear theory [12].

Within this mass region, the most extensively studied and structurally significant nucleus is ^{12}C - a key nucleus for nuclear clustering and stellar nucleosynthesis. The Hoyle state at E_x = 7.65 MeV is a well-known example of a dilute three-α configuration and plays a crucial

*Corresponding author: e-mail: desa.jelavic@irb.hr

© The Authors, published by EDP Sciences. This is an open access article distributed under the terms of the Creative Commons Attribution License 4.0 (https://creativecommons.org/licenses/by/4.0/).

role in helium burning in stars [13]. In addition to the Hoyle state, numerous excited states of ^{12}C have been interpreted in terms of rotational excitations and molecular-like configurations, including triangular and linear-chain geometries [14, 15]. Extending experimental information on high-spin and high-lying states remains important for testing these interpretations and for completing the spectroscopy of cluster configurations in ^{12}C.

The addition of a single valence neutron leads naturally to the neighboring ^{13}C nucleus, providing an opportunity to study how clustering phenomena evolve with increasing neutron number. At low excitation energies, the structure of ^{13}C is reasonably well described within the shell model, while at higher energies cluster configurations such as ^{9}Be+α become increasingly important [16]. Particular interest has been devoted to states that may be related to the Hoyle configuration in ^{12}C, where the valence neutron is weakly coupled to a three-α core [17, 18]. The observation of rotational bands with large moments of inertia, including proposed $K = 3/2^-$ bands, further points to pronounced deformation and molecular-like structures near and above the α-decay threshold [19, 20].

Among structural studies in the $A \approx 10$ mass region, mirror nuclei play an important role as a sensitive probe of nuclear structure. Differences between the excitation spectra of mirror partners directly reflect the interplay between Coulomb effects and the spatial properties of nuclear states. In an idealized picture of isospin symmetry, mirror nuclei are expected to exhibit nearly identical level schemes, apart from an approximately constant Coulomb displacement energy. Deviations from this behavior provide information on the spatial extension of the wave functions and on the balance between Coulomb and nuclear interactions [42]. Since the seminal works of Ehrman and Thomas [22, 23], it has been recognized that weakly bound or spatially extended states may exhibit reduced mirror energy differences, commonly referred to as the Thomas–Ehrman shift. This effect has been discussed for resonant states, cluster configurations, and deformed structures, making mirror spectroscopy a useful tool for identifying spatially extended states in light nuclei [25, 43].

A systematic comparison of several mirror pairs populated under identical experimental conditions therefore provides a direct means of disentangling Coulomb and structural effects and of identifying cluster configurations that may otherwise be difficult to access experimentally [26]. The symmetric ^{10}B+^{10}B reaction is particularly well suited for addressing these questions. The ^{10}B nucleus is one of the few stable nuclei with both an odd number of protons and neutrons and has a relatively high ground-state spin, $J^\pi = 3^+$. Its ground-state structure, which includes significant cluster admixtures of the type ^{6}Li+α, favors the population of high-spin and high-excitation-energy states in a variety of reaction channels [12, 27]. When used symmetrically as both projectile and target, the ^{10}B+^{10}B reaction provides access to nuclei in the $A \approx 10$ region through transfer, pickup, and breakup processes under favorable kinematic conditions, enabling simultaneous studies of mirror nuclei as well as cluster states in ^{12}C and ^{13}C.

2 ^{10}B + ^{10}B experiment

The measurements were performed at the INFN–Laboratori Nazionali del Sud (LNS) in Catania, Italy. A highly focused ^{10}B beam was delivered by the SMP Tandem accelerator at beam energies of 50.0 and 72.2 MeV, impinging on self-supporting ^{10}B targets enriched to 99.8%. While data were collected at both energies, the results discussed in this work are primarily based on the 72.2 MeV measurement, which provided superior statistics and access to higher excitation energies and higher-spin states.

Reaction products were detected using a highly segmented charged-particle detection system consisting of four ΔE–E silicon telescopes. Each telescope was composed of a thin ΔE detector (57–67 μm), divided into four quadrants, followed by a thick double-sided silicon

strip detector (DSSSD) with a thickness of 500 or 1000 μm. Several detector configurations were employed during the experiment, with the polar angles of the telescope centers covering the range from approximately 20° to 53°. A schematic top-view of the reaction chamber and detector arrangement is shown in Fig. 1, illustrating the azimuthal placement of the telescopes around the beam axis.

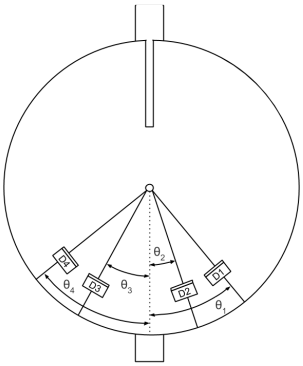


Figure 1. Top-view schematic of the experimental setup, showing the reaction chamber and the arrangement of the four ΔE–E silicon telescopes around the ^{10}B target. The telescopes were positioned at different azimuthal angles and polar angles between $\sim$ 20° and 53° to optimize coverage for various reaction channels.

Further details of the experimental setup, calibration procedures, efficiency corrections, and data analysis methods can be found in Refs. [26, 28, 29] and in the author's PhD thesis [30].

3 Results for mirror nuclei

3.1 $A = 9$: ^{9}Be - ^{9}B

The inclusive excitation-energy spectra of the mirror nuclei ^{9}Be and ^{9}B, reconstructed from the detected ^{11}C and ^{11}B recoils, are shown in Figs. 2 and 3. In both cases, the low-lying spectra are dominated by well-known states belonging to the ground-state rotational bands.

The analog excitation energies for ^{9}Be and ^{9}B are summarized in Table 3. Despite the more complex experimental background in the ^{9}B spectrum, the excitation energies of the mirror partners show good agreement with previously evaluated data [31] and exhibit clear mirror symmetry. The strongest population occurs for members of the ground-state rotational bands ($3/2^{-}$, $5/2^{-}$, and $7/2^{-}$).

Outside the ground-state bands, only the positive-parity $3/2^{+}$ states around 4.5 MeV are observed in both nuclei. These unnatural-parity states have long posed challenges for theoretical descriptions [32], and their spin-parity assignments remain ambiguous, particularly in ^{9}Be [33–39]. The corresponding ^{9}B state observed here at 4.58 MeV is consistent in energy and width with earlier measurements [40].

At higher excitation energies, strong mirror states are observed at 11.46 MeV in ^{9}Be and 11.59 MeV in ^{9}B. Both exhibit comparable widths of about 600 keV and follow the expected $J(J+1)$ energy systematics, supporting their interpretation as $9/2^{-}$ members of the ground-state rotational bands. The small mirror energy difference ($\sim$130 keV) is consistent with Coulomb displacement effects expected for compact configurations, rather than with a Thomas–Ehrman-type shift.

Overall, the excitation spectra of ^{9}Be and ^{9}B display pronounced mirror symmetry for both low-lying and high-spin states. The observed systematics provide important constraints for theoretical models of clustering and rotational motion in light nuclei, while highlighting the sensitivity of mirror spectroscopy to underlying nuclear structure.

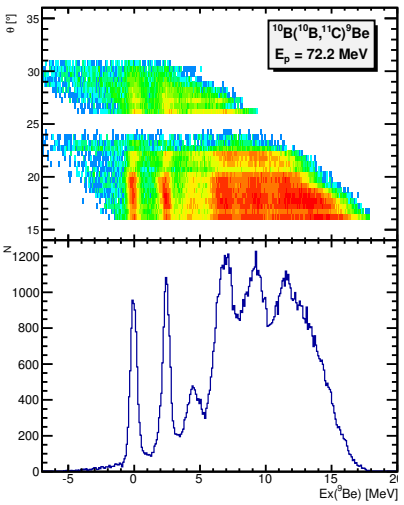


Figure 2. Excitation-energy reconstruction of ^{9}Be using detected ^{11}C recoils. (*Top*) Angular–energy correlation (θ vs. E_x). (*Bottom*) Resulting excitation-energy spectrum of ^{9}Be.

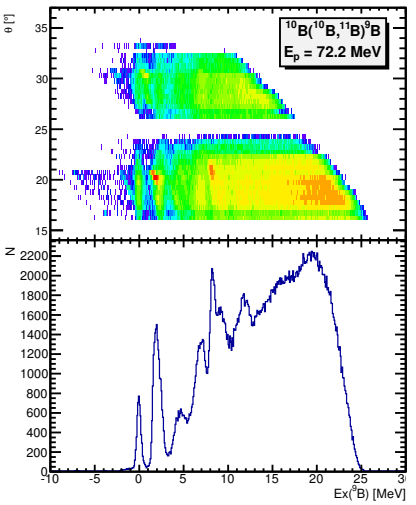


Figure 3. Excitation-energy reconstruction of ^{9}B using detected ^{11}B recoils. (*Top*) Angular–energy correlation (θ vs. E_x). (*Bottom*) Resulting excitation-energy spectrum of ^{9}B.

Table 1. Comparison of excitation energies for the $A = 9$ mirror pair ^{9}Be - ^{9}B. For each nucleus, two columns are shown: excitation energies determined in this work and corresponding values taken from Ref. [31].

J^π	E_x (^{9}Be) [MeV]	E_x(^{9}Be) [MeV][31]	E_x (^{9}B) [MeV]	E_x(^{9}B) [MeV][31]
$3/2^-$	0.00	g.s.	0.00	g.s.
$5/2^-$	2.48	2.429	2.32*	2.361
$(3/2)^+$	4.45	4.704	4.58	4.3
$7/2^-$, $9/2^+$	6.89	6.38, 6.76	6.85	6.97
$(9/2^-)$	11.46	11.283	11.59	11.65

3.2 $A = 10$: ^{10}Be–^{10}C

We now turn to the $A = 10$ mirror system, where the ^{10}B, ^{10}Be, and ^{10}C nuclei provide a well-defined framework for studying mirror symmetry and isobaric analogue states. Figure 4 shows the inclusive excitation-energy spectrum of ^{10}B obtained by detecting the recoil ^{10}B nucleus populated through elastic and inelastic scattering channels. The upper panels display the angular dependence of the reconstructed excitation energy, which aids in separating genuine ^{10}B excitations from background contributions.

The structures labeled 1–3 in the lower panel of Fig. 4 are identified as contributions from elastic and inelastic scattering of ^{10}B on ^{12}C, ^{16}O, and ^{184}W (present in the target in small amounts due to the manufacturing process), respectively. These features do not correspond to intrinsic excitations of ^{10}B and are therefore treated as background components in the analysis. The spectrum is dominated by strong population of the ground state and by a broad structure around 6.12 MeV, which results from the overlap of three closely spaced states with $J^\pi = 2^+$, 4^+, and 3^- at excitation energies of 5.92, 6.025, and 6.127 MeV.

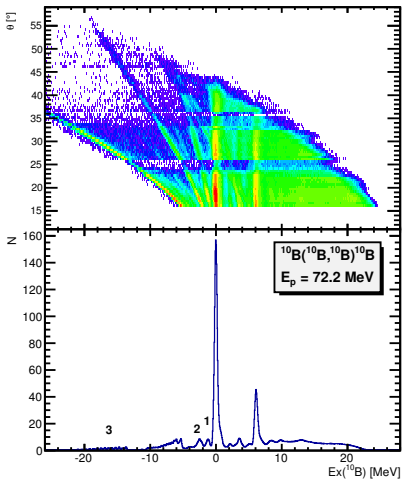


Figure 4. Elastic and inelastic scattering of ^{10}B on a ^{10}B target, including contributions from target impurities, at a beam energy of 72.2 MeV. (*Top*) Polar angle dependence of the excitation energy, shown as a θ vs $E_x(^{10}\mathrm{B})$ distribution. (*Bottom*) Excitation spectrum of ^{10}B. Peaks labeled 1–3 correspond to scattering on nuclei in the target other than ^{10}B.

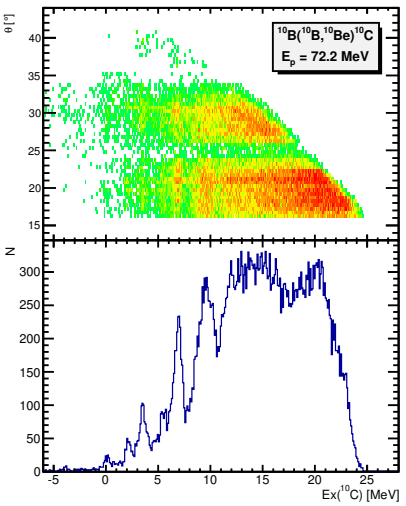


Figure 5. Excitation-energy reconstruction of ^{10}C using detected ^{10}Be recoils. (*Top*) Angular–energy correlation (θ vs. E_x). (*Bottom*) Resulting excitation-energy spectrum of ^{10}C.

After careful background modeling and subtraction, additional weaker excitations become visible. Among these are several $T = 1$ states, which correspond to isobaric analogues of states in ^{10}Be and mirror states of ^{10}C. The identification of these $T = 1$ excitations in ^{10}B provides essential reference points for the interpretation of the ^{10}Be–^{10}C mirror system and for understanding the population mechanisms in the ^{10}B + ^{10}B reaction.

For the $A = 10$ mirror pair, the excitation spectrum of ^{10}C was reconstructed from the detected ^{10}Be recoils following the ^{10}B + ^{10}B reaction. The fitted spectrum (Fig. 5) exhibits several well-known $T = 1$ states reported previously [26, 41], and in addition reveals a previously unreported level at $E_x = 9.24$ MeV. This state appears as a well-isolated structure and cannot be attributed to background contributions or to mutual excitations, as discussed in Ref. [26].

Table 2. Excitation energies for the $A = 10$ mirror nuclei ^{10}Be and ^{10}C, together with the corresponding analogue states observed in ^{10}B. Energies obtained in this work are compared with values from Ref. [41]. For ^{10}B, numbers in parentheses indicate energies relative to the lowest $T = 1$ state at 1.74 MeV.

J^π	^{10}Be [41]	^{10}B	^{10}B [41]	^{10}C	^{10}C [41]
0^+	g.s.	1.78*	1.740 (0.00)	0.00	g.s.
2^+	3.368	5.10	5.164 (3.42)	3.38	3.354
0^+	6.179		7.560 (5.82)	5.32	5.29
3^-,2^+	7.371, 7.542	8.41	8.889, 8.894	6.70	6.55, 6.57
2^+	9.56	9.99	10.84 (9.10)	9.24	

The excitation energy of the newly observed ^{10}C state lies close to that of the established 2^+ state at $E_x = 9.56$ MeV in ^{10}Be [41], suggesting a mirror relationship. The corresponding Coulomb energy difference follows the general systematics observed for most analogue states in the ^{10}Be–^{10}C pair and is consistent with compact configurations [42, 43]. This behavior contrasts with that of the second 0^+ state, which exhibits a significantly larger mirror energy shift and has been interpreted as arising from a more spatially extended structure [26, 44].

The excitation energies of the populated states in ^{10}Be, ^{10}B, and ^{10}C are summarized in Table 2. Overall, the present results demonstrate a high degree of mirror symmetry for the majority of the observed states in the $A = 10$ system, while at the same time illustrating the sensitivity of mirror energy differences to the underlying nuclear structure [26, 42].

3.3 $A = 11$: ^{11}B–^{11}C

Excited states of the mirror nuclei ^{11}B and ^{11}C were populated in the ^{10}B+^{10}B reaction through one-nucleon transfer channels. In the case of ^{11}B, states populated via the ^{10}B(^{10}B,^{9}B)^{11}B reaction were identified by reconstructing the particle-unstable ^{9}B ground state from its decay into two α particles and a proton using triple-coincidence and missing-mass techniques [30]. This approach enables access to complex decay topologies and to states that are difficult to observe in inclusive measurements.

Several known states in ^{11}B are clearly populated, including a high-lying level at $E_x = 11.21$ MeV, observed for the first time in a one-nucleon transfer reaction. For comparison, the excitation spectrum of ^{11}C populated via the ^{10}B(^{10}B,^{9}Be)^{11}C channel exhibits corresponding analogue states. The excitation energies of the populated levels in the two nuclei, summarized in Table 3, show small mirror energy differences consistent with standard Coulomb displacement effects expected for relatively compact configurations. A detailed discussion of the population mechanisms and mirror systematics for the ^{11}B–^{11}C pair, together with spectra, can be found in Ref. [26].

Table 3. Excitation energies for the $A = 11$ mirror nuclei ^{11}B and ^{11}C. All states listed form mirror pairs, with excitation energies obtained in this work compared to literature values from Ref. [45].

J^π	$E_x(^{11}\mathrm{B})$ [MeV]	$E_x(^{11}\mathrm{B})$ [MeV] [45]	$E_x(^{11}\mathrm{C})$ [MeV]	$E_x(^{11}\mathrm{C})$ [MeV][45]
$3/2^-$	0.00	g.s.	0.00	g.s.
$1/2^-$	2.27	2.125	1.97	2.0
$5/2^-$	4.34	4.445	4.32	4.319
$3/2^-$	4.89	5.020	4.84	4.804
$7/2^-$	6.64	6.742	6.48	6.478
$5/2^-$, $7/2^+$	9.02	8.92, 9.18	8.59	8.420, 8.654
$9/2^+$	11.21	11.272	10.69	10.679

4 Results for ^{12}C and ^{13}C

4.1 ^{12}C

Excited states of ^{12}C were investigated through double- and triple-α coincidence measurements following the ^{10}B + ^{10}B reaction. The use of coincidence techniques allows a clean reconstruction of the ^{12}C excitation energy while providing sensitivity to different decay paths and underlying structures.

The excitation-energy spectrum of ^{12}C reconstructed from two-α coincidences, with the additional requirement that the detected α particles originate from the decay of the ^{8}Be ground

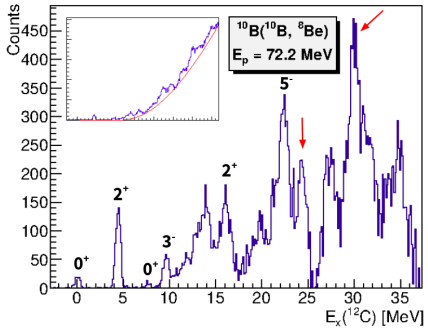


Figure 6. ^{12}C excitation-energy spectrum obtained from two-α coincidence measurements gated on the ^{8}Be ground-state decay. The inset shows the spectrum prior to background subtraction. Red arrows indicate states at 24.4 and 30.3 MeV.

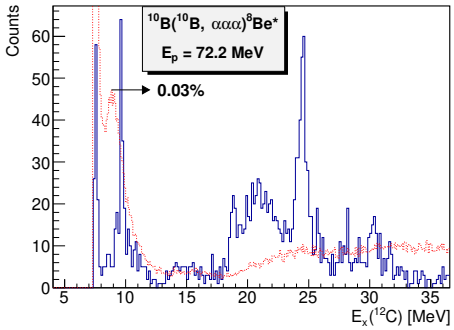


Figure 7. Excitation-energy spectrum of ^{12}C reconstructed from triple-α coincidences. The dotted line represents the Monte Carlo detection efficiency as a function of excitation energy.

state, is shown in Fig. 6. The spectrum is dominated by well-known low-lying states, including the 3^- state at 9.64 MeV and the Hoyle state at 7.65 MeV, although neither of these states is strongly enhanced in this decay channel.

At higher excitation energies, several pronounced structures are observed. In this channel, enhanced population is observed for members of the rotational band associated with a triangular three-α configuration with D_{3h} symmetry, as proposed in Refs. [15, 46]. Members of this band are clearly visible in the present data, indicating the sensitivity of the two-α coincidence channel to these collective excitations.

In the high-excitation-energy region, the spectrum is dominated by the state at E_x = 30.3 MeV, which appears as the most prominent structure. This state has been previously reported and discussed in terms of a highly excited cluster configuration [47]. In addition, a distinct peak corresponding to the state at E_x = 24.4 MeV is observed, as indicated by the red arrow in Fig. 6. While this state is clearly populated, its relative intensity is smaller than that observed in the triple-α coincidence spectrum, shown in Fig. 7.

The excitation-energy spectrum obtained from triple-α coincidences (Fig. 7) emphasizes states that decay through more complex multi-α configurations. Compared to the two-α spectrum, the relative population of individual states is markedly different, demonstrating the strong selectivity of the decay channel. In particular, the state at E_x = 24.4 MeV is strongly populated in triple-α coincidences, while its contribution in the two-α spectrum is significantly weaker.

The enhanced population of the 24.4 MeV state in the triple-α channel points to a decay mechanism involving a simultaneous or near-simultaneous breakup into three α particles, consistent with a highly excited cluster configuration. In this respect, the decay behavior of the 24.4 MeV state shows notable similarities to that of the well-known 3^- state at 9.64 MeV, which is also strongly populated in multi-α decay channels and is commonly interpreted as having a pronounced cluster character [14, 29].

In the present data, both states are preferentially populated in coincidence channels that emphasize multi-α correlations, while they are much less prominent in decay paths dominated by sequential processes. The 24.4 MeV state shows clear similarities to the well-known 3^-

state, in particular in the way it appears in coincidence measurements. For both states, the population is strongly enhanced in the triple-α channel, whereas the contribution in the two-α spectrum is significantly weaker (and similar when accounting for the efficiency). This points to a related decay pattern and possibly to a similar underlying structure of the states discussed.

Taken together, the present results indicate that coincidence selectivity is essential for accessing the structure of highly excited states in ^{12}C and confirm that the ^{10}B+^{10}B reaction provides a suitable tool for populating such states.

4.2 ^{13}C

Excited states of ^{13}C were populated in the ^{10}B+^{10}B reaction primarily through transfer channels leading to ^{9}Be+α final states. Coincidence measurements allow a clean reconstruction of the ^{13}C excitation energy and provide enhanced sensitivity to cluster configurations involving a ^{9}Be core and an α particle.

The excitation-energy spectrum shown in Fig. 8 exhibits a pronounced structure at approximately $E_x \approx 19$ MeV. This state is consistently observed across different detector combinations and stands out clearly above the surrounding background, indicating a genuine ^{13}C excitation rather than a contribution from competing reaction channels. In addition to the coincidence data, the same 19 MeV state is also visible in the inclusive excitation spectrum of ^{13}C reconstructed by detecting ^{7}Be in one of the telescopes [28].

Strong population of the 19 MeV state in the ^{9}Be+α coincidence channel indicates that this state decays predominantly through this configuration at high excitation energy. The fact that the same structure is also observed in the inclusive ^{13}C spectrum gives additional confidence that it corresponds to a genuine ^{13}C excitation, rather than being a channel-specific artifact. Similar cluster-related states in this energy region have been discussed in earlier studies of ^{13}C [48, 49].

Overall, the present data extend the available experimental information on highly excited states in ^{13}C. They also show that the combined use of coincidence and inclusive measurements is important for identifying and confirming cluster-dominated configurations in neutron-rich carbon isotopes.

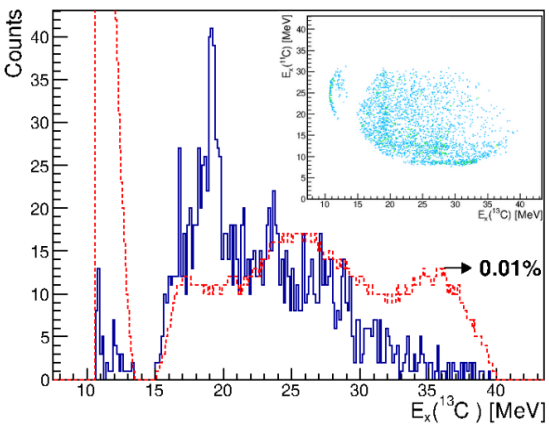


Figure 8. Excitation-energy spectra of ^{13}C reconstructed from α+^{9}Be coincidence events. The dotted line displays the corresponding Monte Carlo detection efficiency. The inset shows a relative-energy (pseudo-Dalitz) plot used to discriminate ^{13}C states from ^{11}C contributions [28].

5 Conclusions

Using the symmetric ^{10}B+^{10}B reaction, a coherent study of clustering and mirror symmetry in the $A \approx 10$ mass region has been performed. The reaction provides efficient population of high-spin and high-excitation-energy states under identical experimental conditions, allowing a systematic comparison of excitation spectra in several mirror pairs as well as in the key cluster nuclei ^{12}C and ^{13}C.

For the mirror systems ^{9}Be - ^{9}B, ^{10}Be - ^{10}C, and ^{11}B - ^{11}C, the observed excitation energies show a high degree of mirror symmetry. Low-lying and high-spin rotational states exhibit mirror energy differences consistent with compact configurations, with few exceptions showing enhanced mirror energy shifts in the populated states. These results provide important constraints on the structure of rotational bands and on the spatial extent of the underlying configurations.

In ^{12}C, the present data confirm the strong population of the state at $E_x = 24.4$ MeV, observed consistently in multi-α coincidence channels. Its selective population and decay properties support its interpretation as a cluster-dominated configuration at high excitation energy. The ability to populate this state efficiently highlights the suitability of the ^{10}B+^{10}B reaction for accessing highly excited cluster states that are difficult to study with other reaction mechanisms.

For ^{13}C, several states near and above the α-decay threshold are populated, including structures associated with ^{9}Be+α configurations. The observation of these states, together with their decay patterns, supports the presence of molecular-like structures and rotational sequences with large moments of inertia.

Overall, the present work demonstrates that the ^{10}B+^{10}B reaction is a powerful tool for simultaneous studies of mirror symmetry and clustering in light nuclei. The combined results provide new experimental benchmarks for theoretical models describing deformation, clustering, and isospin effects in the $A \approx 10$ mass region.

References

[1] N. Ikeda, K. Tagikawa, H. Horiuchi, Prog. Theor. Phys. Suppl. extra num. (1968).
[2] W. von Oertzen, M. Freer and Y. Kanada-En'yo, Phys. Rep. **432**, 43 (2006)
[3] J.P. Ebran, E. Khan, T. Nikšić, D. Vretenar, Nature **487**, 341 (2012)
[4] I. Lombardo, D. Dell'Aquila, Riv. Nuovo Cim. **46**, 521 (2023)
[5] W. von Oertzen, Z. Phys. A **354**, 37 (1996).
[6] M. Freer, Rep. Prog. Phys. **70**, 2149 (2007).
[7] M. Freer *et al.*, Rev. Mod. Phys. **90**, 035004 (2018).
[8] E. Epelbaum *et al.*, Phys. Rev. Lett. **109**, 252501 (2012).
[9] M. Freer *et al.*, Phys. Rev. C **90**, 054324 (2014).
[10] H. Horiuchi et al., Nuclear Physics A **616** 394 (1997).
[11] Y. Kanada-Enyo, H. Horiuchi, A. Dote, Phys. Rev. C 60, 064304 (1999).
[12] P. Navrátil *et al.*, Phys. Rev. Lett. **99**, 042501 (2007).
[13] F. Hoyle, Astrophys. J. Suppl. **1**, 121 (1954).
[14] M. Freer *et al.*, Phys. Rev. C **80**, 041303(R) (2009).
[15] D. Marín-Lámbarri *et al.*, Phys. Rev. Lett. **113**, 012502 (2014).
[16] D. J. Millener *et al.*, Nucl. Phys. A **413**, 1 (1984).
[17] Y. Funaki *et al.*, Eur. Phys. J. A **24**, 321 (2005).
[18] Y. Kanada-En'yo, Phys. Rev. C **86**, 061301(R) (2012).

[19] M. Milin and W. von Oertzen, Eur. Phys. J. A **14**, 295 (2002).
[20] N. Furutachi *et al.*, Phys. Rev. C **83**, 021303(R) (2011).
[21] M. A. Bentley and S. M. Lenzi, Prog. Part. Nucl. Phys. **59**, 497 (2007).
[22] J. B. Ehrman, Phys. Rev. **81**, 412 (1951).
[23] R. G. Thomas, Phys. Rev. **88**, 1109 (1952).
[24] H. T. Fortune and R. Sherr, Phys. Rev. C **73**, 064302 (2006).
[25] Y. Kanada-En'yo, Phys. Rev. C **81**, 034321 (2010).
[26] D. Jelavić Malenica *et al.*, Phys. Rev. C **112**, 044302 (2025).
[27] S. Cohen and D. Kurath, Nucl. Phys. **73**, 1 (1965).
[28] D. Jelavić Malenica *et al.*, Eur. Phys. J. A **59**, 228 (2023).
[29] D. Jelavić Malenica *et al.*, Phys. Rev. C **99**, 064318 (2019).
[30] D. Jelavić Malenica, PhD thesis, University of Zagreb (2015).
[31] D. R. Tilley *et al.*, Nucl. Phys. A **745**, 155 (2004).
[32] F. D. Adler, Nucl. Phys. **78**, 257 (1966).
[33] R. G. Clark *et al.*, Nucl. Phys. A **116**, 97 (1968).
[34] C. E. Jain, Phys. Rev. **123**, 1385 (1961).
[35] J. R. Reeves, Nucl. Phys. A **174**, 129 (1971).
[36] J. A. Deitch *et al.*, Phys. Rev. C **44**, 2159 (1991).
[37] J. L. Glick *et al.*, Phys. Rev. C **43**, 1740 (1991).
[38] A. Arima *et al.*, Nucl. Phys. A **604**, 89 (1996).
[39] H. Iwasaki *et al.*, Phys. Rev. Lett. **115**, 182502 (2015).
[40] A. M. Puckett *et al.*, Phys. Rev. C **32**, 1903 (1985).
[41] D. R. Tilley *et al.*, Nucl. Phys. A **745**, 155 (2004).
[42] M. A. Bentley and S. M. Lenzi, Prog. Part. Nucl. Phys. **59**, 497 (2007).
[43] H. T. Fortune, Phys. Rev. C **73**, 064302 (2006).
[44] M. Ito, EPJ Web Conf. **117** 06014 (2016).
[45] J. H. Kelley, E. Kwan, J. E. Purcell, C. G. Sheu and H. R. Weller, Nucl. Phys. A **880**, 88 (2012).
[46] R. Bijker and F. Iachello, Phys. Rev. Lett. **112**, 152501 (2014).
[47] Đ. Miljanić *et al.*, Nucl. Phys. A **404**, 329 (1983).
[48] N. Soić et al., Nucl. Phys. A **728**, 12 (2003)
[49] I. Lombardo, D. Dell'Aquila, G. Spadaccini, G. Verde, M. Vigilante, Phys. Rev. C **97**, 034320 (2018)